Clinical Neurophysiology 130 (2019) 997–1007

Contents lists available at ScienceDirect

Clinical Neurophysiology

journal homepage: www.elsevier.com/locate/clinph

Acute cerebellar stroke and middle cerebral artery stroke exert distinctive modifications on functional cortical connectivity: A comparative study via EEG graph theory

Fabrizio Vecchio [a,*,1], Pietro Caliandro [b,*,1], Giuseppe Reale [c], Francesca Miraglia [a], Francesca Piludu [e], Gianvito Masi [c], Chiara Iacovelli [f], Chiara Simbolotti [b], Luca Padua [d], Edoardo Leone [e], Francesca Alù [a], Cesare Colosimo [e], Paolo Maria Rossini [b,c]

[a] Brain Connectivity Laboratory, IRCCS San Raffaele Pisana, Rome, Italy
[b] Unità Operativa Complessa di Neurologia, Fondazione Policlinico Universitario A. Gemelli IRCCS, Rome, Italy
[c] Institute of Neurology, Area of Neuroscience, Catholic University of The Sacred Heart, Rome, Italy
[d] Unità operativa di neuroriabilitazione ad alta intensità, Fondazione Policlinico Universitario A. Gemelli. IRCCS, Roma
[e] Department of radiologic sciences, Catholic University, Fondazione Policlincio Universitario A. Gemelli, Rome, Italy
[f] IRCCS Fondazione Don Carlo Gnocchi, Milan, Italy

ARTICLE INFO

Article history:
Accepted 13 March 2019
Available online 6 April 2019

Keywords:
Graph theory
Stroke
Functional connectivity
EEG
Cerebellum
eLORETA
MRI
Lesion volume
Precision medicine

HIGHLIGHTS

- Acute cerebellar stroke may determine changes in brain network architecture.
- Optimal network structure is essential for proper information processing in the brain.
- Functional abnormalities of the brain are found to be associated with the pathological changes in connectivity and network structures.

ABSTRACT

Objective: We tested whether acute cerebellar stroke may determine changes in brain network architecture as defined by cortical sources of EEG rhythms.
Methods: Graph parameters of 41 consecutive stroke patients (<5 days from the event) were studied using eLORETA EEG sources. Network rearrangements of stroke patients were investigated in delta, alpha 2, beta 2 and gamma bands in comparison with healthy subjects.
Results: The delta network remodeling was similar in cerebellar and middle cerebral artery strokes, with a reduction of *small-worldness*. Beta 2 and gamma *small-worldness*, in the right hemisphere of patients with cerebellar stroke, increase respect to healthy subjects, while alpha 2 *small-worldness* increases only among patients with a middle cerebral artery stroke.
Conclusions: The network remodeling characteristics are independent on the size of the ischemic lesion. In the early post-acute stages cerebellar stroke differs from the middle cerebral artery one because it does not cause alpha 2 network remodeling while it determines a high frequency network reorganization in beta 2 and gamma bands with an increase of *small-worldness* characteristics.
Significance: These findings demonstrate changes in the balance of local segregation and global integration induced by cerebellar acute stroke in high EEG frequency bands. They need to be integrated with appropriate follow-up to explore whether further network changes are attained during post-stroke outcome stabilization.

1. Introduction

Functional neuroimaging techniques mainly based on blood flow/metabolism has been repeatedly used to investigate

* Corresponding author at: Brain Connectivity Laboratory, IRCCS San Raffaele Pisana, Via Val Cannuta, 247, 00166 Rome, Italy.
E-mail address: francesca.miraglia@sanraffaele.it (F. Miraglia).
[1] These authors equally contributed to the present manuscript.

https://doi.org/10.1016/j.clinph.2019.03.017
1388-2457/

post-stroke brain plasticity. However, few studies analyzed how location and size of focal ischemic brain lesions in the acute stages could modulate topological properties of widely distributed neural networks (Carrera and Tononi, 2014). In this direction, recent studies investigating network topology highlighted functional reorganization after stroke (Carter et al., 2010; Yin et al., 2014), suggesting that changes in the spontaneous functional architecture of the brain connectivity and constrain clinical output and eventual recovery could be produced by ischemic lesions (Siegel et al., 2016). Recently, the complexity of cerebral functional connectivity has been described through graph theory, a mathematical approach that models the whole brain as an intricate agglomeration of networks with nodes and edges characterized by global integration and local specialization (Tononi et al., 1994; Stam and Reijneveld, 2007; Miraglia et al., 2017), respectively measured as Characteristic path length (L_w) and Clustering coefficient (C_w). A *small-world* network reproduces the competence of the brain networks to process locally and globally the flow of information (Watts and Strogatz, 1998). In this regard, it has been demonstrated via EEG graph analysis that an ischemic stroke is responsible for a bi-hemispheric brain network rearrangement showing a frequency-dependent modality (Caliandro et al., 2017). While the plasticity alterations induced by hemispheric strokes have already been described in terms of anatomical, functional and effective connectivity changes, the brain modifications due to an acute ischemic cerebellar lesion received less attention (De Vico et al., 2017), although the cerebellum is known to be involved in motor control processes and coordination (Kornhuber, 1978; Ramnani et al., 2001), cognitive functions (Kim et al., 1994), learning and relearning mechanisms (Ivry and Baldo, 1992; Allen et al., 1997), all of them playing a pivotal role in the recovery after stroke. It is noteworthy that the cerebellum and cortical areas are widely anatomically interconnected: as for the anatomical routes, cortico-ponto-cerebellar projections form part of a closed loop system with the cerebral cortex, in which the cerebellum returns projections mainly to the contralateral cerebral cortex –namely the motor one- via the thalamus (Asanuma et al., 1983; Schmahmann and Pandya, 1997; Middleton and Strick, 1997; Ramnani, 2006). In addition, there is also evidence of functional and neurophysiological cortical-cerebellar diaschisis as demonstrated by clinical observations and different experimental settings. In healthy subjects, for instance, the excitability of the contralateral primary motor cortex and posterior parietal cortex could be modulated by the cerebellum (Casula et al., 2016), while in a rodent model of focal ischemia in the cerebral cortex, chronic contralateral cerebellar deep brain stimulation has shown therapeutically effective results as it promotes a plastic perilesional reorganization (Cooperrider et al., 2014). Moreover, in patients with subacute middle cerebral artery (MCA) ischemic stroke, improvements of upper extremity motor recovery were found to

Table 1
Demographic and clinical data of patients.

Patient	Age	Gender	Stroke site	NIHSS acute phase	NIHSS at 3 months	Lesion site
01	56	F	R	14	5	MCA stroke
02	55	M	R	12	LF	MCA stroke
03	70	M	R	1	0	MCA stroke
04	62	M	R	2	0	MCA stroke
05	74	M	R	21	13	MCA stroke
06	87	F	R	12	1	MCA stroke
07	60	M	R	5	1	MCA stroke
08	73	M	R	2	1	MCA stroke
09	62	M	R	4	2	MCA stroke
10	74	M	L	5	dead	MCA stroke
11	49	M	L	19	11	MCA stroke
12	78	M	L	8	8	MCA stroke
13	80	M	L	9	LF	MCA stroke
14	64	F	L	4	2	MCA stroke
15	75	M	L	10	0	MCA stroke
16	81	F	L	24	13	MCA stroke
17	56	F	L	18	3	MCA stroke
18	66	M	L	7	L.F.	MCA stroke
19	62	M	L	4	3	MCA stroke
20	74	M	L	4	3	MCA stroke
21	75	M	L	6	3	MCA stroke
22	52	M	L	13	6	MCA stroke
23	63	M	L	5	3	MCA stroke
24	63	M	L	2	0	MCA stroke
25	67	M	R	16	9	MCA stroke
26	82	M	L	15	11	MCA stroke
27	72	M	L	22	11	MCA stroke
28	63	F	L	9	7	MCA stroke
29	44	M	L	19	7	MCA stroke
30	80	F	L	1	5	MCA stroke
31	76	M	L	3	dead	Cerebellar stroke
32	73	M	L	2	0	Cerebellar stroke
33	46	F	L	1	0	Cerebellar stroke
34	58	M	L	3	2	Cerebellar stroke
35	65	F	L	4	1	Cerebellar stroke
36	79	F	L	6	4	Cerebellar stroke
37	38	F	L	3	1	Cerebellar stroke
38	75	M	L	4	1	Cerebellar stroke
39	73	F	R	1	0	Cerebellar stroke
40	80	F	R	3	1	Cerebellar stroke
41	45	F	L	2	0	Cerebellar stroke

be predicted by increased MEG-recorded functional connectivity of alpha band in the perilesional area and in the whole cerebellum (Westlake et al., 2012).

Given these premises, which together demonstrate a mutual influence between the cerebellum and the cerebral cortex, we hypothesize that acute cerebellar ischemia may induce rearrangements of the cerebral functional networks as explored via graph theory on EEG signals. If it be so, on the basis of the considerations made above, we verified whether these rearrangements differ from those related to MCA territory stroke and, *a latere*, we evaluated whether the lesion volume may influence functional connectivity rearrangements.

2. Patients and methods

Forty-one stroke patients (mean age 66.5, SD 11.9, 27 males and 14 females) in the MCA territory or in the cerebellum were consecutively recruited within 5 days from symptoms onset. Exclusion criteria were previous ischemic stroke and hemorrhage. We clinically assessed the patients by the National Institutes of Health Stroke Scale (NIHSS) during the acute phase and three months later. Demographic and clinical data of the patients are reported in Table 1. All patients were right-handed (Salmaso and Longoni, 1985) as showed by Handedness Questionnaire. The study was approved by the local Ethical Committee in conformity to the Declaration of Helsinki and national guidelines. Informed consent was acquired. Furthermore, we studied 30 healthy subjects, age- and sex-matched, as controls.

2.1. Control analyses

As a control analysis, power spectral densities and power topographies were evaluated to rule out that all connectivity effects were not confounded by differences in spectral power. These power density spectra (PSD) were evaluated by the use of sLORETA method (Pascual-Marqui, 2002). We computed intracranial spectral density, from EEG normalized data epochs to cortical current density time series at 6239 cortical voxels, with a resolution of 0.5 Hz, from 0.5 to 45 Hz. sLORETA is a standardized linear, discrete, minimum norm, method that solves the inverse problem to reconstruct the 3D cortical distribution of the neuronal sources activity from EEG data recorded on the scalp. The sLORETA standardization allows tomography of standardized current density with exact localization, although with low spatial resolution (i.e. the neighboring neuronal sources are highly correlated) (see Pascual-Marqui, 2002 for a review). It was demonstrated (Pascual-Marqui, 2009) that sLORETA has exact and zero-error localization property and has no localization bias even with biological noise (Greenblatt et al., 2005; Sekihara et al., 2005). The power density spectra were evaluated in all patients and the comparisons among areas were addressed.

We have analyzed power spectra of patients in 6 Regions Of Interest (ROIs) for each hemisphere. The ROIs were defined according to the BAs and corresponded to the following regions: central, temporal, frontal, occipital, parietal, and limbic areas.

2.2. Recordings and preprocessing of EEG data

Electroencephalographic signals were measured in eyes closed resting state condition (at least 5 minutes) from 19 electrodes in the International 10–20 system position. To monitor eye movements were recorded horizontal and vertical EOGs. Impedances between skin and electrode were maintained below 5 KΩ and the sampling rate fixed at 256 Hz.

EEG data were analyzed with Matlab software (MathWorks, Natick, MA) and using scripts implemented in EEGLAB toolbox. Data were band-pass filtered with a finite impulse response (FIR) filter from 0.2 to 47 Hz. To eliminate artifactual interferences (i.e. ocular, muscular, cardiac etc), imported data were fragmented in 2 sec epochs and the epochs with aberrant waveforms were removed by an expert EEGer (no patient presented epileptiform activity). Then, the rejection of artifacts were finalized with Independent Component Analysis (ICA) through Infomax ICA algorithm (Bell and Sejnowski, 1995; Vecchio et al., 2014b). It is a blind source decomposition algorithm that allows the statistically independent sources separation from multichannel data. It was demonstrated as an effective method for separating eye movements artifacts from EEG data (Jung et al., 2000; Iriarte et al., 2003; Hoffmann and Falkenstein, 2008). For the analyzed patients group, the average number of artifact-free epochs was 138 (±13.33 SE).

2.3. EEG connectivity analysis

Functional connectivity of EEG data were carried out with eLORETA (Pascual-Marqui et al., 2011; Vecchio et al., 2014a; Vecchio et al., 2014c; Vecchio et al., 2015; Tecchio et al., 2016) software. eLORETA algorithm is a linear inverse solution for detection of EEG signals source. eLORETA method was validated by several studies, due to its improved localization properties. As important note, the deep structures, such as the mesial temporal lobes (Zumsteg et al., 2006) and the anterior cingulate cortex (Pizzagalli et al., 2001) can be properly localized with the method. The computation of EEG sources was made using the MNI152 template (Mazziotta et al., 2001), in a realistic head model (Fuchs et al., 2002) with the 3D solution space limited to cortical gray matter, as defined by the probabilistic Talairach atlas (Lancaster et al., 2000). Intracerebral volume is divided in 6239 voxels with a resolution 5 mm spatially. Therefore, eLORETA tomography is the electric activity at each voxel in MNI space and represents the estimated current density magnitude. The Brodmann areas are used as anatomical labels and are also extracted from MNI space, corrected by Talairach space (Brett et al., 2002). As a general limitation of the current study approach, it should be reported the low number of EEG channels and the not perfect reconstruction of the head model in lesioned brain.

Brain connectivity was obtain by eLORETA software in 84 regions located in the center of the Brodmann Areas of the affected (ipsilesional) and unaffected (contralesional) hemispheres. The aforementioned Brodmann Areas represented our Regions of Interest (ROIs). Each cortical signal ROI represents the average electric neuronal activities of all voxels belonging to that ROI, as obtained by eLORETA.

In each hemisphere it was computed intracortical Lagged Linear Coherence (Pascual-Marqui, 2007; Pascual-Marqui et al., 2011) between the eLORETA current density time series of all the possible pairs of ROIs for EEG frequency bands. For each subject, it were evaluated delta (2–4 Hz), theta (4–8 Hz), alpha 1 (8–10.5 Hz), alpha 2 (10.5–13 Hz), beta 1 (13–20 Hz), beta 2 (20–30 Hz) and gamma (30–45 Hz) bands.

"Lagged linear coherence was developed as an accurate measure of the physiological connectivity, being not affected by volume conduction and low spatial resolution" (Pascual-Marqui, 2007; Pascual-Marqui et al., 2011). Lagged linear connectivity values estimated among all the possible pairs of ROIs for each frequency band and in both hemispheres were used as weights of the graph analysis as follows.

Below, we briefly summarize the core concepts of graph theory but encourage the interested Reader to the relative references for a more deepening. They were computed the graph theory measures that represent the concepts of network segregation and network

integration. Brain segregation is the network tendency to be organized in clusters and is computed by the clustering coefficient (*C*); the brain integration represents the network ability to exchange information between distant regions and is obtain by the characteristic path length (*L*) parameter (Watts and Strogatz, 1998; Miraglia et al., 2016). In the current study, undirected and weighted brain networks were designed. The nodes of the network are represented by the BAs and the edges are weighted by lagged linear connectivity values (Miraglia et al., 2015).

In a weighted graph, the clustering coefficient (*Cw*) and the characteristic path length (*Lw*) are defined from Onnela and colleagues (Onnela et al., 2005; Rubinov and Sporns, 2010).

The *small-world* (*Sw*) coefficient is commonly described as a balance between the local connections and the global integrations in a network. It was obtain through the ratio between *Cw* and *Lw* (Watts and Strogatz, 1998; Rubinov and Sporns, 2010). When *Sw* is bigger than 1, a network has *small-world* properties, with short path length and high clustering coefficient.

For each subject, *Cw* and *Lw* values of each band are normalized with the average values of *Cw* and *Lw* computed in all the frequency bands.

2.4. MRI procedures

Within the clinical frame of diagnostic procedures and to evaluate whether cortical connectivity modifications were influenced by the ischemic lesion volume, all patients underwent to a 1.5-T MRI scan (Philips Achieva, Best, The Netherlands) with an eight-channel phased-array neurovascular coil to obtain fluid-attenuated inversion recovery (FLAIR), diffusion-weighted imaging (DWI), turbo spin echo (TSE), a gradient echo (GRE) magnetic resonance angiography and images of intracranial arteries.

DWI was obtained by a single-shot turbo spin-echo planar imaging technique with repetition time of 6934 ms, echo time of 66 ms, a matrix number of 112 × 89, and two *b* values of 0 and 1000 s/mm^2 and slice thickness of 4 mm. FLAIR image was acquired from a turbo-spin-echo sequence with repetition time/echo time of 8000/120 ms, an inversion time of 2300 ms, a 256 × 181 matrix and a slice thickness of 4 mm. The parameters for acquiring turbo spin echoT1w sequence were repetition time of 597 ms, echo time of 9 ms, a 224 × 175 matrix size and slice thickness of 4 mm.

An expert neuroradiologist manually defined the acute brain ischemic areas. The parenchymal infarction boundary was identified by hyper intense regions in DWIs with b = 1000 s/mm^2, and in FLAIR images. Before contouring, DWIs and FLAIR images were co-registered using rigid body transformations. All sections containing the acute ischemic areas were outlined for each patient. Volumes were then quantified in cm^3; 3D, while Slicer Software was used to visualize and coregister the image sets and to delineate and quantify the lesion volume. In order to obtain a normalized measure of the lesion, for each patient the total intracranial volume was estimated on TSE T1 and FLAIR images with voxel-based morphometry (VBM) using MATLAB 8.1 (the MathWorks, Natick, MA) and Statistical Parametric Mapping (SPM8).

2.5. Statistical evaluation

We used SPSS software package for Windows, release 12.0. The normality of the distributions was investigated by Shapiro-Wilk probability test. In order to compare the PSD of the different ROIs for each frequency band in the two patients groups it was used the Kruskal-Wallis test. The Bonferroni corrected Mann-Whitney test was used for post-hoc pairwise comparisons.

We designed a multiple regression model to investigate if *Sw* for each frequency band was dependent from the covariates: gender, age, NIHSS score in the acute phase and stroke territory (MCA and cerebellar stroke). We defined the three groups (MCA stroke, cerebellar stroke and controls) as dummy variables, being the control subjects scored as 0–0. The hemispheres of patients were matched with ipsilateral hemispheres of controls. R^2 was used to test the goodness of fit of the model. When the regression model explained the variation of *Sw* in a specific frequency, we analyzed the group effect (MCA stroke, cerebellar stroke and controls) on *Cw* and *Lw* values in that frequency by Kruskal-Wallis test with Bonferroni correction for post-hoc pairwise comparisons. Each hemisphere of patients was compared with the ipsilateral hemisphere of controls. We used Mann–Whitney U test to analyze the group effect on age and NIHSS score. Sex distribution among groups was evaluated by the chi-square test.

In order to evaluate the correlation between the ischemic lesion volume and *Sw* of both hemispheres for those frequencies significant at multiple regression model the Spearman test was used. Moreover, the Spearman test was also used to evaluate the correlation between NIHSS total score at three months and *Sw* indexes significant at multiple regression analysis. The alpha level was considered at $p < 0.05$.

3. Results

We enrolled 30 patients with ACM stroke (mean age 67.3, SD 10.61, 23 males and 7 females) and 11 with cerebellar stroke (mean age 64.36, SD 15.18, 4 males and 7 females). Cerebellar and ACM stroke patients did not differ in age, while sex distribution was different between the two samples (p:0.02 see Table 1). Cerebellar patients presented a less severe clinical picture than ACM patients both in the acute phase (NIHSS total score median value was 3 range 1–6 in cerebellar and 9 range 1–24 in ACM patients p:0.001) and in the follow up (NIHSS total score median value was 1 range 1–4 in cerebellar and 3 range 0–13 in ACM patients p:0.005). NIHSS total score variation at three months did not differ between the two groups.

3.1. Power density spectra analysis

In the ACM group Kruskal-Wallis test showed a difference among ROIs in delta and alpha1 bands (respectively p:0.009 and p:0.02). The post-hoc analysis showed that delta band PSD of the right limbic area is lower than PSD in left frontal area (p: 0.0001) no difference between pairs was found for alpha1 PSD. In the cerebellar group, Kruskal-Wallis test showed no difference among ROIs. In the two groups of patients no difference was found between the homologous ROIs in both hemispheres and in each frequency band.

With illustrative purposes, we reported the grand averaged power spectra of the ROIs for both hemispheres in the two patients groups (Figs. 1 and 2) and in a couple of paradigmatic stroke patients (Figs. 3 and 4).

3.2. Small-world differences between cerebellar stroke, MCA territory stroke and healthy subjects

Results of the regression model results are reported in Table 2. *Sw* for each frequency band was not dependent from the covariates age, gender, NIHSS score in the acute phase. Acute cerebellar ischemia was accompanied with significant modifications of the cerebral functional networks. Brain connectivity changes were mostly founded in delta, beta 2 and gamma bands: namely, a bilateral reduced of S_w in delta band and an increased of S_w in beta 2 and gamma bands in the right hemisphere. Likewise, MCA territory stroke patients showed a similar pattern of cortical connectivity

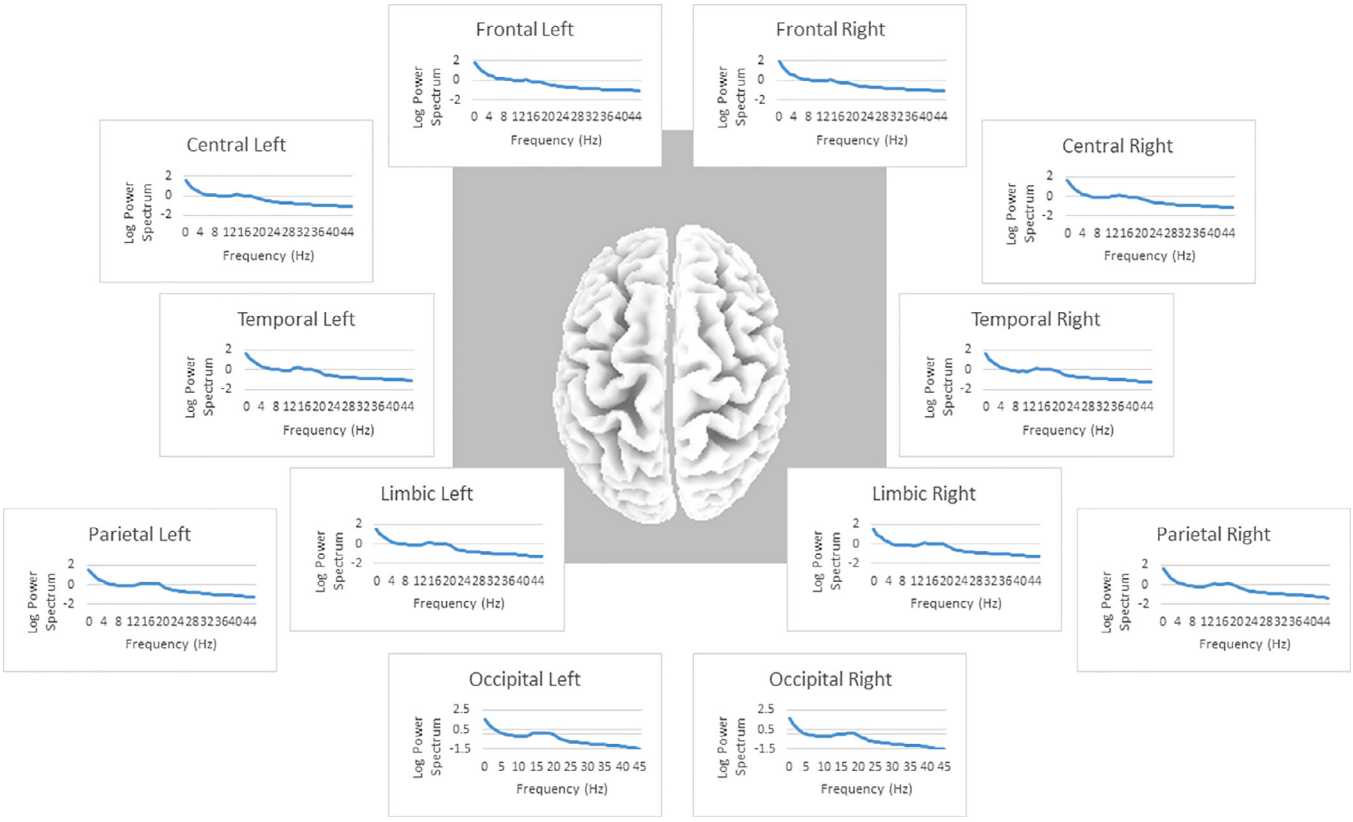

Fig. 1. Power spectra of the ROIs considered in the statistical analysis for both hemispheres in the grand average of all medial patients.

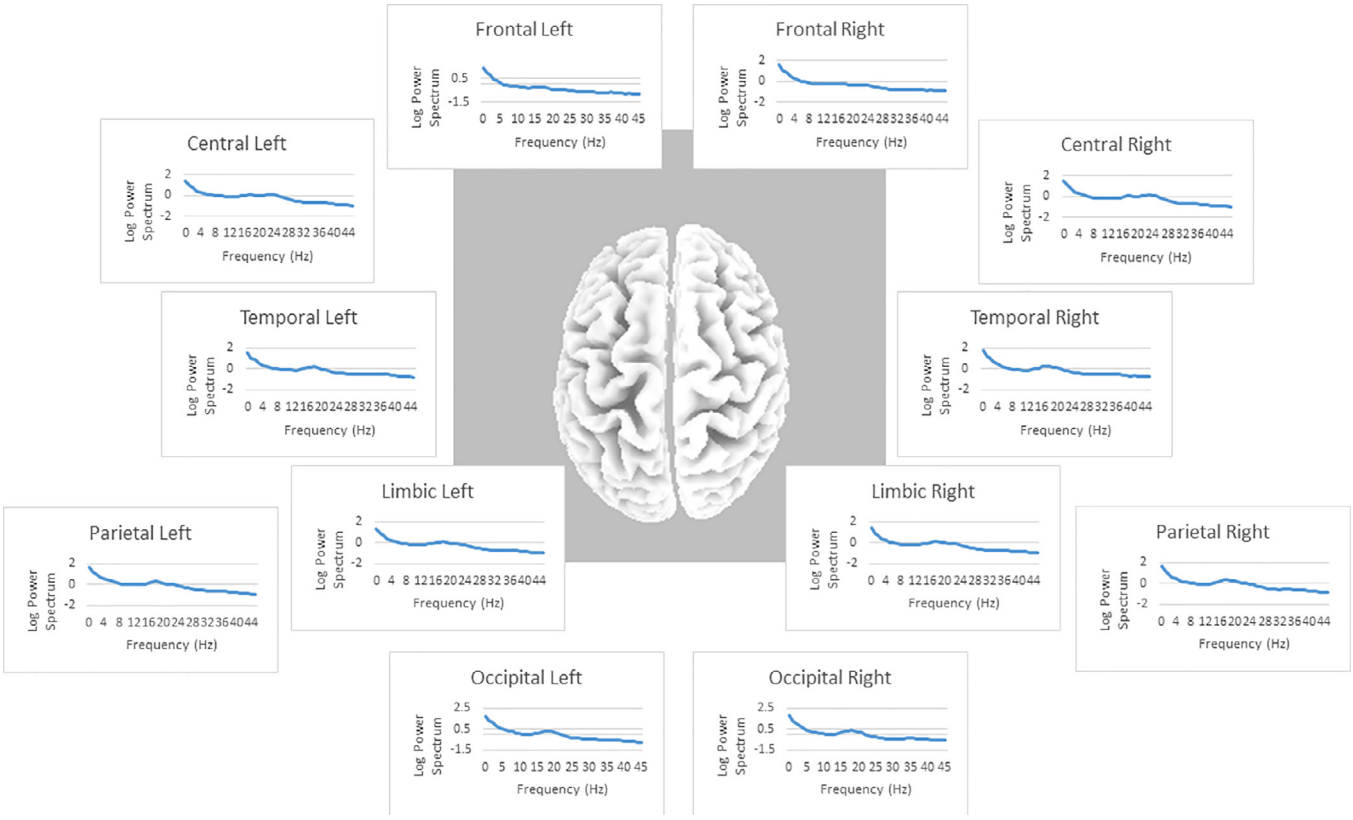

Fig. 2. Power spectra of the ROIs considered in the statistical analysis for both hemispheres in the grand average of all posterior patients.

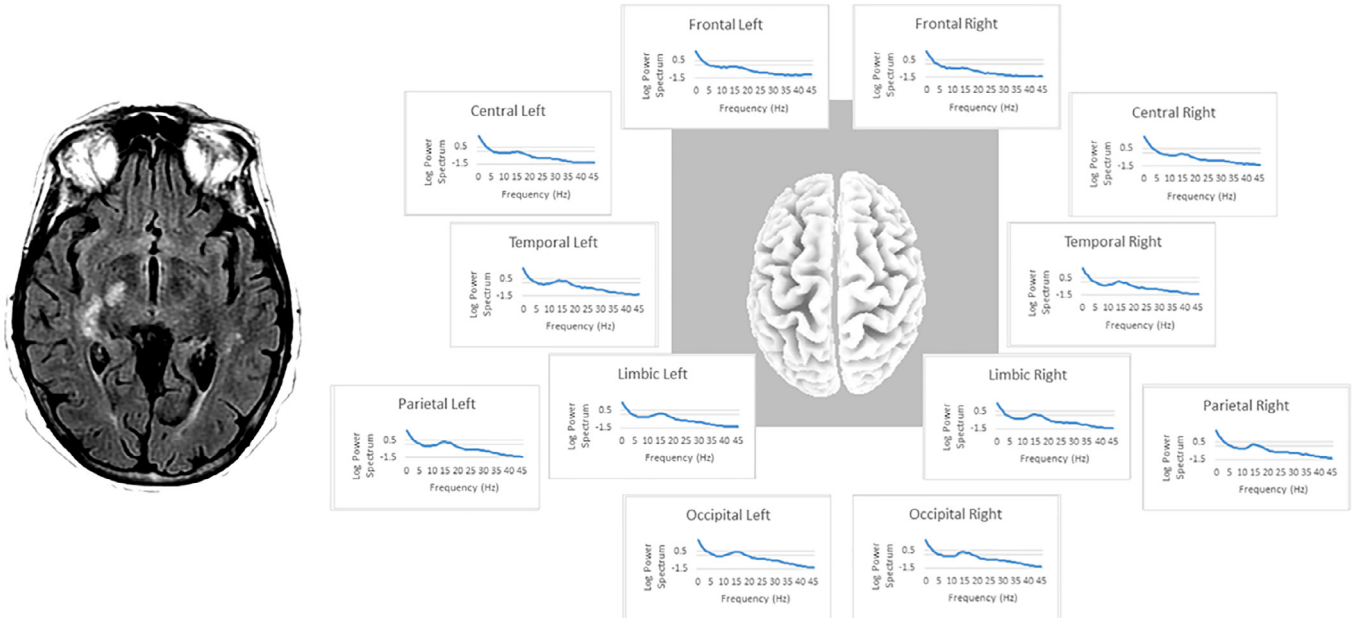

Fig. 3. Power spectra of the ROIs considered in the statistical analysis for both hemispheres in a paradigmatic medial stroke patients.

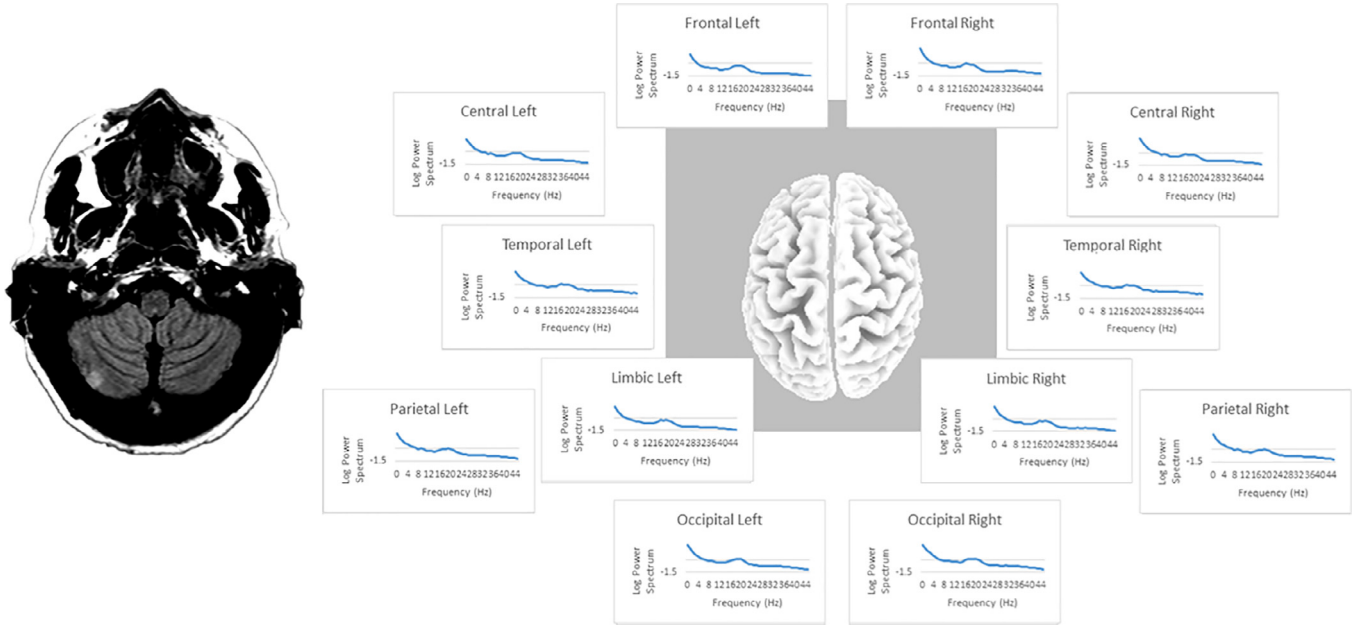

Fig. 4. Power spectra of the ROIs considered in the statistical analysis for both hemispheres in a paradigmatic posterior stroke patients.

changes when delta band was taken into account, but no statistically significant differences were observed in beta 2 and gamma bands, like the former group. Conversely, as already described in a previous study (Caliandro et al., 2017) MCA territory stroke was also characterized by a bihemispheric increased S_w in alpha 2 band. Fig. 5 summarizes the Sw data in frequency bands statistically significant in the regression model. Fig. 6 shows the connectivity spectra (based on lagged linear coherence values) in the same frequency bands. The *Sw* values of statistically significant frequency bands do not correlate with the ischemic lesion volume and with the total score of NIHSS at 3 months both in MCA and cerebellar stroke patients. Fig. 7 shows the connectivity matrices in two representative cerebellar patients with different lesion volume.

3.3. Clustering and path length differences

No statistically significant differences were found between cerebellar stroke patients and the normative group regarding C_w and L_w in delta, beta 2 and gamma frequencies for each hemisphere. On the other hand, MCA territory stroke was associated with higher C_w ($p = 0.01$for right hemisphere and $p = 0.02$ for left hemisphere) and a higher L_w ($p = 0.007$ for right hemisphere and $p = 0.02$ for left hemisphere) in delta band of both hemispheres compared to controls, meaning respectively greater segregation and lower integration. Furthermore, either hemispheres were characterized by lower C_W ($p = 0.003$ and $p = 0.004$ respectively for the right and left hemisphere) and lower L_W ($p = 0.003$ and $p = 0.002$ for right and left hemispheres) in alpha 2 band, resulting

Table 2
Results of the regression model adopted for each hemisphere network. The bold character refers to significant values.

Variables	Delta S_w		Theta S_w		Alpha 1 S_w		Alpha 2 S_w		Beta 1 S_w		Beta 2 S_w		Gamma S_w	
	Right Hem	Left Hem	Right Hem	Left Hem	Right Hem	Left Hem	Right Hem	Left Hem	Right Hem	Left Hem	Right Hem	Left Hem	Right Hem	Left Hem
Age	0.107	0.154	−0.107	−0.012	0.025	−0.116	−0.206	−0.220	−0.203	−0.052	−0.081	0.001	0.081	0.080
	(0.370)	(0.195)	(0.438)	(0.927)	(0.859)	(0.396)	(0.112)	(0.077)	(0.132)	(0.702)	(0.540)	(0.994)	(0.543)	(0.558)
Gender	0.052	0.066	0.059	0.080	−0.040	0.173	0.012	−0.109	0.121	−0.081	0.030	−0.104	0.027	−0.093
	(0.659)	(0.575)	(0.668)	(0.557)	(0.772)	(0.205)	(0.922)	(0.375)	(0.361)	(0.546)	(0.820)	(0.439)	(0.841)	(0.496)
NIHSS	0.181	−0.004	0.158	0.053	−0.067	0.288	0.042	0.000	−0.052	−0.169	−0.160	−0.174	−0.152	−0.184
total score	(0.254)	(0.978)	(0.387)	(0.769)	(0.718)	(0.116)	(0.804)	(1.000)	(0.768)	(0.348)	(0.361)	(0.333)	(0.394)	(0.313)
MCA	**−0.631**	**−0.475**	−0.334	−0.333	−0.128	−0.289	**0.338**	**0.448**	0.017	0.318	0.207	0.294	0.208	0.192
stroke	**(<0.001)**	**(0.004)**	(0.071)	(0.070)	(0.489)	(0.116)	**(0.04)**	**(0.008)**	(0.924)	(0.082)	(0.240)	(0.105)	(0.242)	(0.294)
Cerebellar	**−0.237**	**−0.283**	−0.057	−0.007	−0.188	−0.064	0.180	0.141	0.265	0.223	**0.362**	0.258	**0.354**	0.242
stroke	**(0.04)**	**(0.021)**	(0.682)	(0.957)	(0.182)	(0.641)	(0.168)	(0.258)	(0.053)	(0.106)	**(0.008)**	(0.062)	**(0.011)**	(0.084)
R^2	0.313	0.316	0.082	0.093	0.061	0.092	0.198	0.267	0.134	0.108	0.157	0.116	0.134	0.089

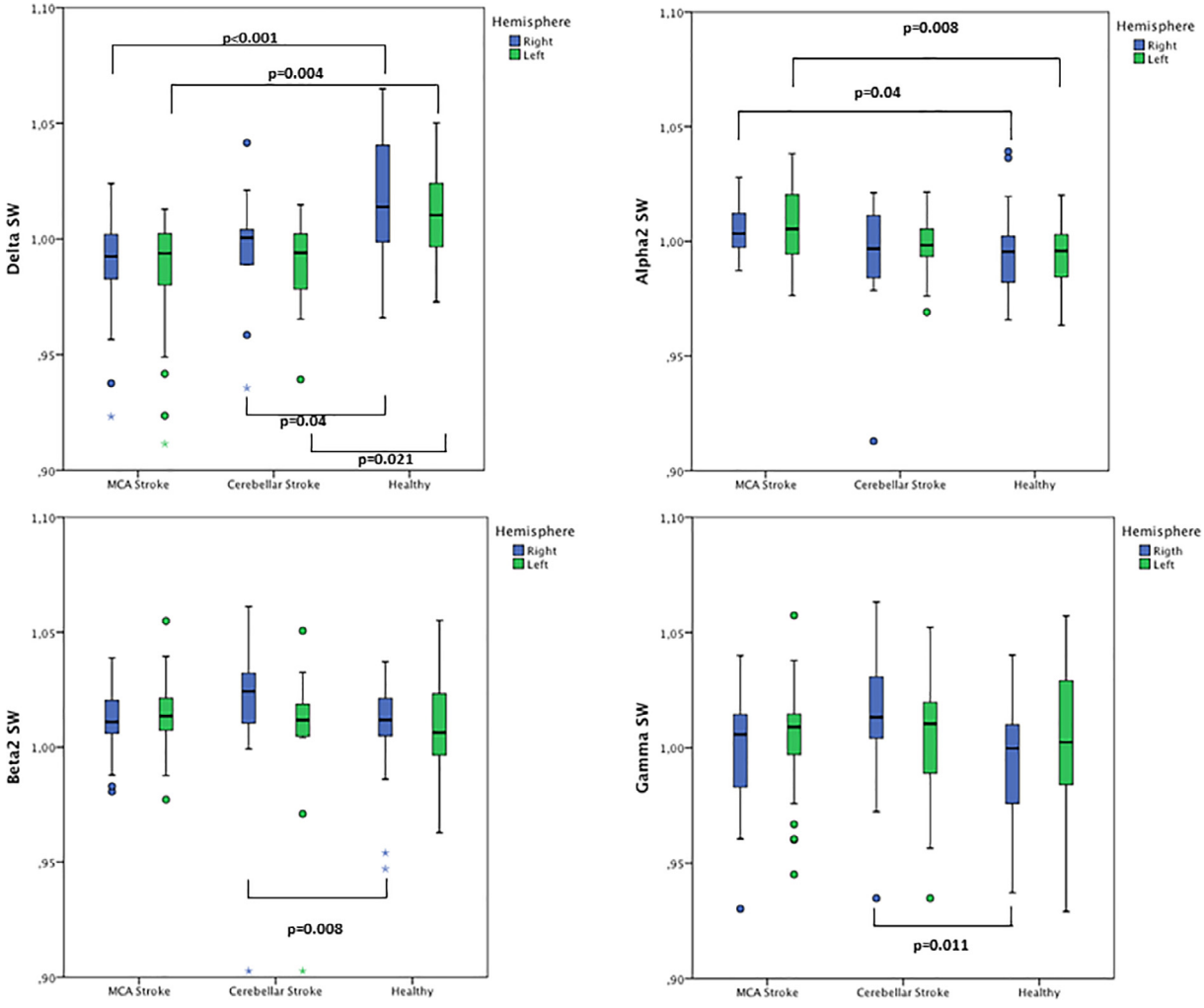

Fig. 5. Summarizes the Sw data in frequency bands statistically significant in the regression model. The box plots show the median values, first and third quartile (respectively bottom and top of the box), range (I), outliers (°) and extremes (*).

respectively in a lesser brain segregation and a greater cerebral integration.

4. Discussion

First of all, it is important to point out that our study was conducted to verify whether acute cerebellar stroke could determine any change on resting-state brain functional connectivity.

In fact, different studies have revealed that the outputs from the cerebellum influence widespread regions of the cerebral cortex: not only does the cerebellum send dense projections to the motor thalamus (VAL) (Aumann et al., 1994; Teune et al., 2000), but it also reflects to the posterior thalamic nucleus, reciprocally linked to the primary motor and sensory cortices, and to the intralaminar nuclei, more specifically engaged across cortical areas in the coordination of activity (Jones, 2001).

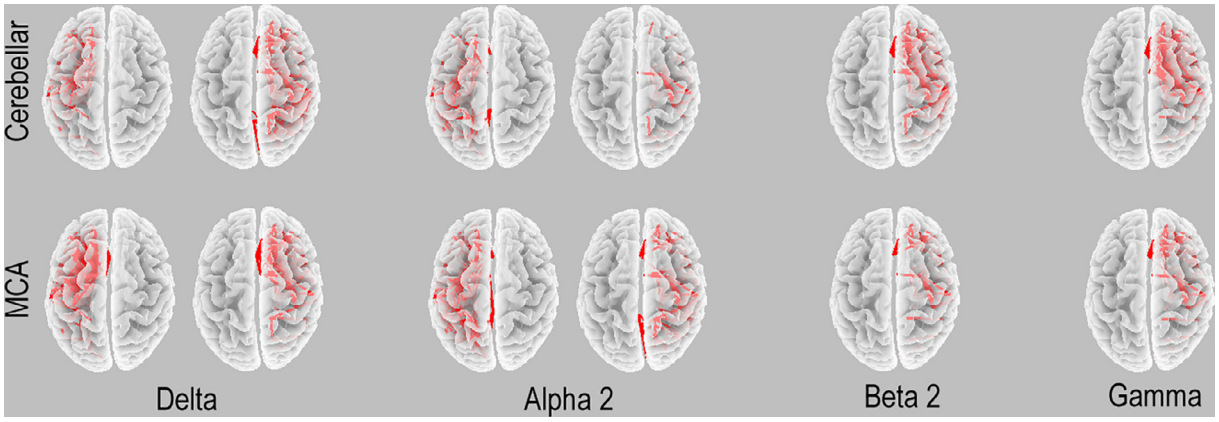

Fig. 6. eLORETA connectivity maps for delta, alpha 2, beta 2 and gamma bands, in the two groups of patients. Each red tract, among the 42 ROIs of each hemisphere, refers to the connectivity value higher than the cut-off threshold. (For interpretation of the references to colour in this figure legend, the reader is referred to the web version of this article.)

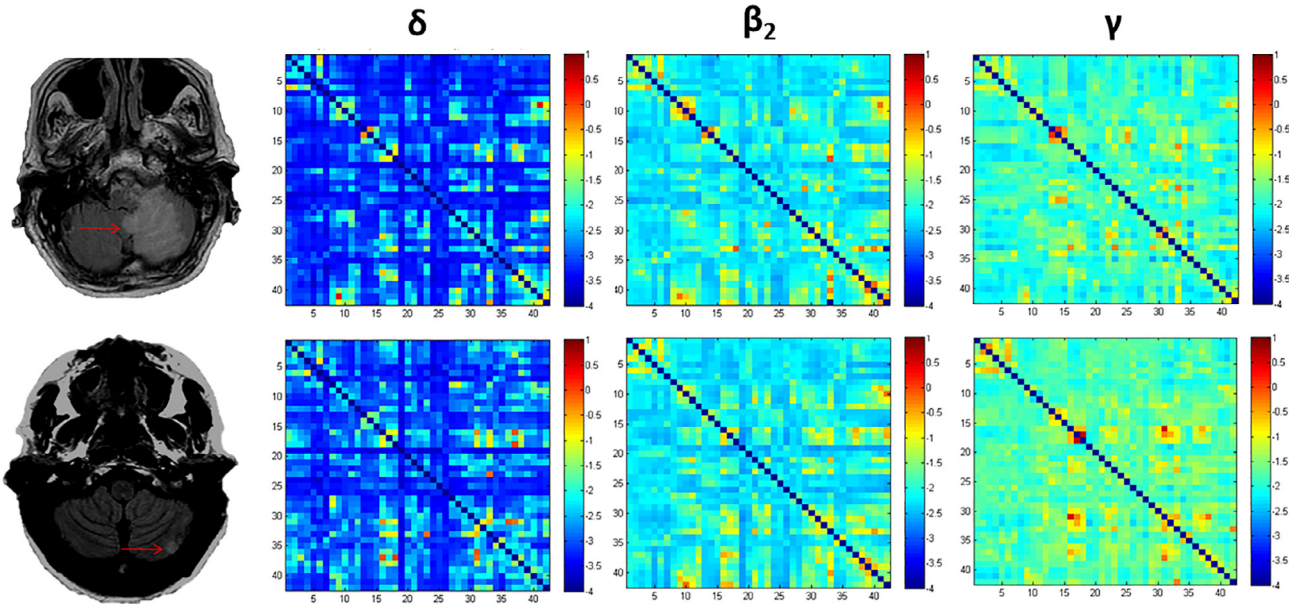

Fig. 7. Shows the connectivity matrices of right hemisphere (based on lagged linear coherence values) in two representative left cerebellar stroke patients with different lesion volume.

As hypothesized on the basis of the anatomical and functional links between the cerebellum and the neocortex, acute cerebellar ischemia is able to exert significant modifications on the cortical brain networks in a frequency-dependent modality. Indeed, connectivity changes of eyes closed resting-state functional network were mainly detected in both low- and high- frequency EEG bands: namely, in delta, beta 2 and gamma, while no network rearrangement was found in theta, alpha 1, alpha 2 and beta 1. We observed a bi-hemispheric decreased *small-worldness* in delta band and a right-hemispheric increased *small-worldness* in beta 2 and gamma bands. In the MCA stroke patients we found similar findings in delta band as well; furthermore, a bilaterally increased *small-worldness* was found in alpha 2 band. In view of the above, it is notable that cerebellar and MCA stroke network remodeling share an analogous low frequency connectivity pattern but they exhibit a different one in higher EEG frequencies. We believe that differences in connectivity are not confounded by differences in power spectra (Voytek and Knight, 2015; Haller et al., 2018). In fact, our analysis demonstrates no difference in PSD between homologous ROIs of the two hemispheres of patients in each frequency band although, in cerebellar patients, a clear difference was observed between right and left hemisphere in terms of connectivity in beta 2 and gamma bands.

Our results enhance the evidence about the role of cerebellum in influencing cortical network connectivity of EEG signals in a frequency-dependent modality probably by modifying the functional cerebello-thalamo-cortical balance of mutual control (Aumann et al., 1994; Teune et al., 2000; Jones, 2001). Regarding the low EEG frequencies, to the best of our knowledge this is the first time that delta network *Sw* modifications after a cerebellar stroke are described. Having the delta rhythm both a thalamic (Villablanca and Salinas-Zeballos, 1972; Ball et al., 1977) and cortical (Steriade et al., 1993; Timofeev and Chauvette, 2011) generators, and considering the wide cerebellum-cortex anatomical connection via the thalamus, a reduction of cerebellar output to thalamus could interfere with the functional connection between the cortical and thalamic delta generators. It is to emphasize that either MCA or cerebellar stroke induces a bilateral reduction of hemispheric delta *Sw* meanings a less efficient balance between local segregation and global integration. In MCA stroke patients

delta power is bilaterally enhanced (Assenza et al., 2009; Wu et al., 2016) and the increase of delta activity in the contralateral hemisphere could reflect a dysfunctional state provoked by a lack of inputs from the affected hemisphere (Butefisch et al., 2008) causing an increase of spontaneous oscillating activity of contralateral cortical neurons (Topolnik et al., 2003). Alternatively, the increased delta activity could be related to a reduced intracortical inhibition in the unaffected hemisphere, a sort of compensative mechanism which finally ends-up with an increased excitability useful for recruitment of 'silent' synapses and networks for an action vicariating the lost function (Shimizu et al., 2002; Manganotti et al., 2008). Bearing in mind the similarity in delta *Sw* changes in MCA and cerebellar stroke, we may speculate that interhemispheric disconnections and/or impaired intracortical inhibition can be involved in bilateral cortical delta changes through cerebellum-thalamus pathway dysfunction (Rastogi et al., 2017; Schulz et al., 2017).

It is worth emphasizing that our study provides evidence of cerebellar modulation of cortical electrical activity, showing a role for the cerebellum in the control of resting-state cortical gamma-band connectivity. The presence of intrinsic gamma generators has been demonstrated in the neocortex (Cardin et al., 2009; Whittington et al., 2011), in the thalamus (Timofeev and Steriade, 1997) and in the cerebellum (Whittington et al., 2011); more specifically, both in neocortex and in cerebellum, gamma activity seems related to the firing of fast-spiking interneurons (Middleton et al., 2008; Cardin et al., 2009). Furthermore, as already described in an animal model (Timofeev and Steriade, 1997) and in healthy humans (Schutter et al., 2003), the aforementioned generators could be modulated by stimulating/disrupting the functional and anatomical links of the cerebello-thalamo-cortical networks. Indeed, stimuli to contralateral deep cerebellar nuclei or superior cerebellar peduncle evoke gamma oscillations in the thalamic ventrolateral nucleus which are coherent in phase with neocortex gamma activity oscillations (Timofeev and Steriade, 1997). Moreover, an experimental lesion in the superior cerebellar peduncle of cat brain determines a reduction/abolition of thalamic gamma rhythmic firing (Timofeev and Steriade, 1997). On the other hand we have to consider that cerebellar stimulation via transcranial magnetic impulses (TMS) can modulate short-interval intracortical inhibition, intracortical facilitation and long-interval intracortical inhibition of the contralateral motor cortex according to the characteristics of the cerebellar stimuli and their effects on the dentato-thalamo-cortical pathway (Koch, 2010). Along this pathway Purkinje cells have inhibitory connections with the deep cerebellar nuclei, which have a disynaptic excitatory connection through the ventral thalamus to the motor cortex. Inhibitory Purkinje cells output results in a reduction of excitatory output from deep cerebellar nuclei to the motor cortex (Eccles et al., 1967; Ito, 2002; Kelly and Strick, 2003). On the basis of the evidences reported above, we can speculate that cerebellar stroke causes an impairment of the cerebellar modulation of the thalamic firing in the gamma frequency range by disrupting the functional connections among Purkinje cells, deep cerebellar nuclei and thalamus which subsequently affects the neocortex functional network itself. The way in which these mechanisms induce a higher gamma *Sw* in acute cerebellar stroke patients need however to be elucidated more deeply.

It is noteworthy that we observed significant high-frequency network modifications only in the right hemisphere. The composition of our sample, where there is a prevalence of left cerebellar stroke, and the decussation of cerebellar output towards neocortex, put together, could explain the network modifications only observed in the right hemisphere. However, another possible explanation is that changes in cerebellar activity determine a left-to-right gamma lateralization regardless the side of cerebellar lesion as also suggested by a previous study in healthy subjects that showed a higher gamma power spectrum in the right prefrontal cortex after high frequency TMS preferentially targeting the medial cerebellum (Schutter et al., 2003). Less we can hypothesize about beta 2 Sw network modification in right hemisphere. We know from the literature that cerebellar theta burst TMS stimulation applied to a cerebellar hemisphere can augment the EEG activity in the beta rhythms spectrum in the contralateral motor cortex (Casula et al., 2016). It is reasonable to hypothesize that the right beta 2 *Sw* modulation could be somehow linked to the composition of our sample, where there is a prevalence of patients with left cerebellar lesion. It is interesting to underline that our findings on increased beta 2 and gamma *Sw* in resting-state condition is similar to those observed in patients with different focal cerebellar lesions during the performance of a finger task (De Vico et al., 2017). De Vico and colleagues found an increased *Sw* in beta 2 and gamma bands during the execution of the task either with the affected or with the unaffected hand and found no correlation between the graph indexes and the clinical picture, specifically the motor performance (ICARS), general intelligence (IQWAIS-R), and Z-cognitive scores. Although the two studies analyse different samples of patients (acute stroke in our study and patients with focal surgical and ischemic lesions in De Vico's manuscript), results are complementary. It is well known that motor connectivity patterns are influenced by movement parameters (Grosse et al., 2002) and therefore the connectivity changes observed during a finger task might theoretically be also determined by the movement and not only related to the focal cerebellar lesion. In our approach, we evaluated the changes in resting state weighted network (therefore without the confounding effect of movement) and found a similar change in beta 2 and gamma *Sw* unequivocally demonstrating that acute cerebellar stroke determines a reorganization of the brain network in beta 2 and gamma bands.

Further studies are needed to better understand the clinical implications of these results. We found that cerebellar patients present a less severe picture than MCA either in the acute phase or at three months follow-up confirming that after focal cerebellar insults recovery is frequent and long-term disability is rare (Kelly et al., 2001). However, our regression model show no relationship between *Sw* and NIHSS total score in the acute phase and the correlation analysis shows no relation between Sw indexes and the clinical severity at three months as measured by NIHSS.

Our results were obtained during recordings of EEG during the early post-stroke stages; they need to be integrated with appropriate follow-up EEG recordings to explore whether further network changes are attained during post-stroke outcome stabilization.

5. Conclusions

Our findings demonstrate that cortical network modifications subsequent to acute stroke in different vascular territories share both analogies and differences. On one hand, both cerebellar and MCA stroke determine a similar remodelling of the delta band network that results in a reduction of small-worldness. On the other hand, cerebellar stroke differs from the MCA one because it does not cause alpha 2 network remodelling while it determines a high frequency network reorganization in beta 2 and gamma band with an increase of *small-worldness*.

Acknowledgements

The article is partially funded by the Italian Ministry of Health ("Ricerca corrente") and "Fondazione Roma" NCDs Call for Proposal 2013: "Post-stroke brain connectivity and functional outcome

following traditional and enhanced neurorehabilitation by non-invasive brain stimulation. Giordano Lacidogna for clinical evaluation.

Conflict of Interest statement

None of the authors have potential conflicts of interest to be disclosed.

References

Allen G, Buxton RB, Wong EC, Courchesne E. Attentional activation of the cerebellum independent of motor involvement. Science 1997;275:1940–3.

Asanuma C, Thach WT, Jones EG. Distribution of cerebellar terminations and their relation to other afferent terminations in the ventral lateral thalamic region of the monkey. Brain Res 1983;286:237–65.

Assenza G, Zappasodi F, Squitti R, Altamura C, Ventriglia M, Ercolani M, et al. Neuronal functionality assessed by magnetoencephalography is related to oxidative stress system in acute ischemic stroke. Neuroimage 2009;44:1267–73.

Aumann TD, Rawson JA, Finkelstein DI, Horne MK. Projections from the lateral and interposed cerebellar nuclei to the thalamus of the rat: a light and electron microscopic study using single and double antero- grade labelling. J Comput Neurol 1994;349:165–81.

Ball GJ, Gloor P, Schaul N. The cortical electromicrophysiology of pathological delta waves in the electroencephalogram of cats. Electroencephalogr Clin Neurophysiol 1977;43:346–61.

Bell AJ, Sejnowski TJ. An information-maximization approach to blind separation and blind deconvolution. Neural Comput 1995;7:1129–59.

Brett M, Johnsrude IS, Owen AM. The problem of functional localization in the human brain. Nat Rev Neurosci 2002;3:243–9.

Butefisch CM, Wessling M, Netz J, Seitz RJ, Homberg V. Relationship between interhemispheric inhibition and motor cortex excitability in subacute stroke patients. Neurorehabil Neural Repair 2008;22:4–21.

Caliandro P, Vecchio F, Miraglia F, Reale G, Della MG, La TG, et al. Small-World characteristics of cortical connectivity changes in acute stroke. Neurorehabil Neural Repair 2017;31:81–94.

Cardin JA, Carlen M, Meletis K, Knoblich U, Zhang F, Deisseroth K, et al. Driving fast-spiking cells induces gamma rhythm and controls sensory responses. Nature 2009;459:663–7.

Carrera E, Tononi G. Diaschisis: past, present, future. Brain 2014;137:2408–22.

Carter AR, Astafiev SV, Lang CE, Connor LT, Rengachary J, Strube MJ, et al. Resting interhemispheric functional magnetic resonance imaging connectivity predicts performance after stroke. Ann Neurol 2010;67:365–75.

Casula EP, Pellicciari MC, Ponzo V, Stampanoni BM, Veniero D, Caltagirone C, et al. Cerebellar theta burst stimulation modulates the neural activity of interconnected parietal and motor areas. Sci Rep 2016;6:36191.

Cooperrider J, Furmaga H, Plow E, Park HJ, Chen Z, Kidd G, et al. Chronic deep cerebellar stimulation promotes long-term potentiation, microstructural plasticity, and reorganization of perilesional cortical representation in a rodent model. J Neurosci 2014;34:9040–50.

De Vico FF, Clausi S, Leggio M, Chavez M, Valencia M, Maglione AG, et al. Interhemispheric connectivity characterizes cortical reorganization in motor-related networks after cerebellar lesions. Cerebellum 2017;16:358–75.

Eccles JC, Ito M, Szentagothai J. The cerebellum as a neuronal machine. Berlin: Springer-Verlag; 1967.

Fuchs M, Kastner J, Wagner M, Hawes S, Ebersole JS. A standardized boundary element method volume conductor model. Clin Neurophysiol 2002;113:702–12.

Greenblatt RE, Ossadtchi A, Pflieger ME. Local linear estimators for the bioelectromagnetic inverse problem. IEEE Trans Signal Process 2005;53:3403–12.

Grosse P, Cassidy MJ, Brown P. EEG-EMG, MEG-EMG and EMG-EMG frequency analysis: physiological principles and clinical applications. Clin Neurophysiol 2002;113:1523–31.

Haller M, Donoghue T, Peterson E, Varma P, Sebastian P, Gao R, et al. Parameterizing neural power spectra. bioRxiv 2018;40.

Hoffmann S, Falkenstein M. The correction of eye blink artefacts in the EEG: a comparison of two prominent methods. PLoS One 2008;3:e3004.

Iriarte J, Urrestarazu E, Valencia M, Alegre M, Malanda A, Viteri C, et al. Independent component analysis as a tool to eliminate artifacts in EEG: a quantitative study. J Clin Neurophysiol 2003;20:249–57.

Ito M. The molecular organization of cerebellar long-term depression. Nat Rev Neurosci 2002;3:896–902.

Ivry RB, Baldo JV. Is the cerebellum involved in learning and cognition? Curr Opin Neurobiol 1992;2:212–6.

Jones EG. The thalamic matrix and thalamocortical synchrony. Trends Neurosci 2001;24:595–601.

Jung TP, Makeig S, Humphries C, Lee TW, McKeown MJ, Iragui V, et al. Removing electroencephalographic artifacts by blind source separation. Psychophysiology 2000;37:163–78.

Kelly PJ, Stein J, Shafqat S, Eskey C, Doherty D, Chang Y, et al. Functional recovery after rehabilitation for cerebellar stroke. Stroke 2001;32:530–4.

Kelly RM, Strick PL. Cerebellar loops with motor cortex and prefrontal cortex of a nonhuman primate. J Neurosci 2003;23:8432–44.

Kim SG, Ugurbil K, Strick PL. Activation of a cerebellar output nucleus during cognitive processing. Science 1994;265:949–51.

Koch G. Repetitive transcranial magnetic stimulation: a tool for human cerebellar plasticity. Funct Neurol 2010;25:159–63.

Kornhuber HH. Cortex, basal ganglia and cerebellum in motor control. Electroencephalogr Clin Neurophysiol Suppl 1978;34:449–55.

Lancaster JL, Woldorff MG, Parsons LM, Liotti M, Freitas CS, Rainey L, et al. Automated Talairach atlas labels for functional brain mapping. Hum Brain Mapp 2000;10:120–31.

Manganotti P, Acler M, Zanette GP, Smania N, Fiaschi A. Motor cortical disinhibition during early and late recovery after stroke. Neurorehabil Neural Repair 2008;22:396–403.

Mazziotta J, Toga A, Evans A, Fox P, Lancaster J, Zilles K, et al. A probabilistic atlas and reference system for the human brain: International Consortium for Brain Mapping (ICBM). Philos Trans R Soc Lond B Biol Sci 2001;356(1412):1293–322.

Middleton FA, Strick PL. Dentate output channels: motor and cognitive components. Prog Brain Res 1997;114:553–66.

Middleton SJ, Racca C, Cunningham MO, Traub RD, Monyer H, Knopfel T, et al. High-frequency network oscillations in cerebellar cortex. Neuron 2008;58:763–74.

Miraglia F, Vecchio F, Bramanti P, Rossini PM. Small-worldness characteristics and its gender relation in specific hemispheric networks. Neuroscience 2015;310:1–11.

Miraglia F, Vecchio F, Bramanti P, Rossini PM. EEG characteristics in "eyes-open" versus "eyes-closed" conditions: Small-world network architecture in healthy aging and age-related brain degeneration. Clin Neurophysiol 2016;127:1261–8.

Miraglia F, Vecchio F, Rossini PM. Searching for signs of aging and dementia in EEG through network analysis. Behav Brain Res 2017;317:292–300.

Onnela JP, Saramaki J, Kertesz J, Kaski K. Intensity and coherence of motifs in weighted complex networks. Phys Rev E Stat Nonlin Soft Matter Phys 2005;71:065103.

Pascual-Marqui RD. Instantaneous and lagged measurements of linear and nonlinear dependence between groups of multivariate time series: frequency decomposition. arXiv preprint arXiv:0711 1455; 2007.

Pascual-Marqui RD. Standardized low-resolution brain electromagnetic tomography (sLORETA): technical details. Methods Find Exp Clin Pharmacol 2002(24 Suppl D):5–12.

Pascual-Marqui RD. Theory of the EEG inverse problem. In: Artech House B, editor. Quantitative EEG analysis: methods and clinical applications; 2009. p. 121–40.

Pascual-Marqui RD, Lehmann D, Koukkou M, Kochi K, Anderer P, Saletu B, et al. Assessing interactions in the brain with exact low-resolution electromagnetic tomography. Philos Trans A Math Phys Eng Sci 2011;369:3768–84.

Pizzagalli DA, Pascual-Marqui RD, Nitschke JB, Oakes TR, Larson CL, Abercrombie HC, et al. Anterior cingulate activity as a predictor of degree of treatment response in major depression: evidence from brain electrical tomography analysis. Am J Psychiatry 2001;158:405–15.

Ramnani N, Toni I, Passingham RE, Haggard P. The cerebellum and parietal cortex play a specific role in coordination: a PET study. Neuroimage 2001;14:899–911.

Ramnani N. The primate cortico-cerebellar system: anatomy and function. Nat Rev Neurosci 2006;7:511–22.

Rastogi A, Cash R, Dunlop K, Vesia M, Kucyi A, Ghahremani A, et al. Modulation of cognitive cerebello-cerebral functional connectivity by lateral cerebellar continuous theta burst stimulation. Neuroimage 2017;158:48–57.

Rubinov M, Sporns O. Complex network measures of brain connectivity: uses and interpretations. Neuroimage 2010;52:1059–69.

Salmaso D, Longoni AM. Problems in the assessment of hand preference. Cortex 1985;21:533–49.

Schmahmann JD, Pandya DN. The cerebrocerebellar system. 1997; 17. Int Rev Neurobiol 1997;41:31–60.

Schulz R, Frey BM, Koch P, Zimerman M, Bonstrup M, Feldheim J, et al. Cortico-cerebellar structural connectivity is related to residual motor output in chronic stroke. Cereb Cortex 2017;27:635–45.

Schutter DJ, van HJ, d'Alfonso AA, Peper JS, Panksepp J. High frequency repetitive transcranial magnetic over the medial cerebellum induces a shift in the prefrontal electroencephalography gamma spectrum: a pilot study in humans. Neurosci Lett 2003;336:73–6.

Sekihara K, Sahani M, Nagarajan SS. Localization bias and spatial resolution of adaptive and non-adaptive spatial filters for MEG source reconstruction. Neuroimage 2005;25:1056–67.

Shimizu T, Hosaki A, Hino T, Sato M, Komori T, Hirai S, et al. Motor cortical disinhibition in the unaffected hemisphere after unilateral cortical stroke. Brain 2002;125:1896–907.

Siegel JS, Ramsey LE, Snyder AZ, Metcalf NV, Chacko RV, Weinberger K, et al. Disruptions of network connectivity predict impairment in multiple behavioral domains after stroke. Proc Natl Acad Sci U S A 2016;113:E4367–76.

Stam CJ, Reijneveld JC. Graph theoretical analysis of complex networks in the brain. Nonlinear Biomed Phys 2007;1:3.

Steriade M, Nunez A, Amzica F. Intracellular analysis of relations between the slow (< 1 Hz) neocortical oscillation and other sleep rhythms of the electroencephalogram. J Neurosci 1993;13:3266–83.

Tecchio F, Vecchio F, Ventriglia M, Porcaro C, Miraglia F, Siotto M, et al. Non-ceruloplasmin copper distinguishes a distinct subtype of alzheimer's disease: a study of EEG-derived brain activity. Curr Alzheimer Res 2016;13:1374–84.

Teune TM, van der Burg J, van der Moer J, Voogd J, Ruigrok TJ. Topography of cerebellar nuclear projections to the brain stem in the rat. Prog Brain Res 2000;124:141–72.

Timofeev I, Steriade M. Fast (mainly 30–100 Hz) oscillations in the cat cerebellothalamic pathway and their synchronization with cortical potentials. J Physiol 1997;504(Pt 1):153–68.
Timofeev I, Chauvette S. Thalamocortical oscillations: local control of EEG slow waves. Curr Top Med Chem 2011;11:2457–71.
Tononi G, Sporns O, Edelman GM. A measure for brain complexity: relating functional segregation and integration in the nervous system. Proc Natl Acad Sci U S A 1994;91:5033–7.
Topolnik L, Steriade M, Timofeev I. Partial cortical deafferentation promotes development of paroxysmal activity. Cereb Cortex 2003;13:883–93.
Vecchio F, Miraglia F, Bramanti P, Rossini PM. Human brain networks in physiological aging: a graph theoretical analysis of cortical connectivity from EEG data. J Alzheimers Dis 2014a;41:1239–49.
Vecchio F, Lacidogna G, Miraglia F, Bramanti P, Ferreri F, Rossini PM. Prestimulus interhemispheric coupling of brain rhythms predicts cognitive-motor performance in healthy humans. J Cogn Neurosci 2014b;26:1883–90.
Vecchio F, Miraglia F, Marra C, Quaranta D, Vita MG, Bramanti P, et al. Human brain networks in cognitive decline: a graph theoretical analysis of cortical connectivity from EEG data. J Alzheimers Dis 2014c;41:113–27.
Vecchio F, Miraglia F, Valeriani L, Scarpellini MG, Bramanti P, Mecarelli O, et al. Cortical brain connectivity and B-type natriuretic peptide in patients with congestive heart failure. Clin EEG Neurosci 2015;46:224–9.
Villablanca J, Salinas-Zeballos ME. Sleep-wakefulness, EEG and behavioral studies of chronic cats without the thalamus: the 'athalamic' cat. Arch Ital Biol 1972;110:383–411.
Voytek B, Knight RT. Dynamic network communication as a unifying neural basis for cognition, development, aging, and disease. Biol Psychiatry 2015;77:1089–97.
Watts DJ, Strogatz SH. Collective dynamics of 'small-world' networks. Nature 1998;393:440–2.
Westlake KP, Hinkley LB, Bucci M, Guggisberg AG, Byl N, Findlay AM, et al. Resting state alpha-band functional connectivity and recovery after stroke. Exp Neurol 2012;237:160–9.
Whittington MA, Cunningham MO, LeBeau FE, Racca C, Traub RD. Multiple origins of the cortical gamma rhythm. Dev Neurobiol 2011;71:92–106.
Wu J, Srinivasan R, Burke QE, Solodkin A, Small SL, Cramer SC. Utility of EEG measures of brain function in patients with acute stroke. J Neurophysiol 2016;115:2399–405.
Yin D, Song F, Xu D, Sun L, Men W, Zang L, et al. Altered topological properties of the cortical motor-related network in patients with subcortical stroke revealed by graph theoretical analysis. Hum Brain Mapp 2014;35:3343–59.
Zumsteg D, Friedman A, Wieser HG, Wennberg RA. Propagation of interictal discharges in temporal lobe epilepsy: correlation of spatiotemporal mapping with intracranial foramen ovale electrode recordings. Clin Neurophysiol 2006;117:2615–26.